JOURNAL OF APPLIED ELECTROCHEMISTRY 17 (1987) 545–551

Gas phase relations for protonic solid-electrolyte fuel cells

J. D. CANADAY, T. A. WHEAT, A. AHMAD, A. K. KURIAKOSE

Ceramic Section, Mineral Processing Laboratory, CANMET, 555 Booth Street, Ottawa, Ontario, Canada K1A 0G1

Received 11 March 1986; revised 19 May 1986

Gas phase relations are applied to a protonic solid-electrolyte fuel cell operating at 300° C. Kinetic theory and diffusion are considered with the electrodes subjected to a static gas pressure. For hydrogen and oxygen flow to the anode and cathode, respectively, gas flow parameters are investigated for this dynamic system. The relative effects of the static and dynamic gases are assessed and it is found that the rate of molecular incidence at the electrode surface from gas flow is insignificant relative to that caused by thermal motion during laminar flow. The implications of this result for fuel cell design are discussed.

Molecular mean free paths are discussed in relation to the electrode morphological parameter of pore size. Diffusion coefficients and corresponding limiting current densities are evaluated for three processes. It is found that for electrodes with 10% porosity the rate-determining steps are caused by activation or ohmic polarization rather than by concentration polarization.

Nomenclature

A	area
D	Fick's law diffusion coefficient
$D_{1,1}$	coefficient for the self-diffusion of like molecules
$D_{1,2}$	coefficient for the interdiffusion of two gas species
D_k	Knudsen diffusion coefficient
d	diameter of gas flow area
F	Faraday's constant
f	volume flow rate at 300° C, 1 atm
f'	volume flow rate as measured by mass flow controller
k	Boltzmann's constant
I	current
J	current density
J_L	limiting current density
J_m	molar flux
M_1	gram molecular weight of gas species one
M_2	gram molecular weight of gas species two
m	molecular mass
N_v	number of moles per unit volume
n	number of molecules per unit volume
n_e	number of electron transfers
P	gas pressure
P_i	partial pressure of gas species
p	porosity
Q	total charge
r	electrode pore radius
R	electrical resistance
Re	Reynolds number
R_g	gas constant
T	gas temperature
t	time
v	linear velocity of gas
$\bar{v}$	average molecular velocity
$\bar{v}_1$	average molecular velocity of species one
$\bar{v}_2$	average molecular velocity of species two
V	gas volume
V_{cell}	cell voltage
V_e	equilibrium voltage
V_{act}	activation polarization
V_{conc}	concentration polarization
z'	number of molecules striking a surface perpendicular to the flow direction per

unit area and time
z number of molecules striking a surface perpendicular to the incident direction per unit time resulting from thermal velocity
δ_1 molecular diameter of species one
δ_2 molecular diameter of species two
$\delta_{1,2}$ average molecular diameter of species one and two
$\lambda_{1,1}$ mean free path between collisions of like molecules
$\lambda_{1,2}$, $\lambda_{2,1}$ mean free path of one species between collisions with a second species
λ_1, λ_2 mean free path for one species when colliding with either species one or two
ϱ mass density
τ tortuosity

1. Introduction

The CANMET fuel cell programme is concerned with the development of solid electrolytes and electrodes. Electrolyte research has been centred on β-Al_2O_3 and Nasicon-type compounds [1–3] in which ionic conductivity occurs through the migration of cationic species such as H^+ and H_3O^+ following an ion exchange process. These protonic materials can be operated in the temperature range 100–300° C, in contrast with the ZrO_2-type electrolytes that require a temperature of 1000° C in order to achieve adequate conductivity. The lower temperature of a protonic cell results in a higher thermodynamic efficiency and fewer problems with materials.

Production of electric power by a fuel cell requires the transport of reactant gases such as hydrogen to the anode and oxygen to the cathode. The interaction of the gas with the electrode may affect the performance of the fuel cell. However, there have been only a limited number of analytical or experimental studies of these effects. The process of Knudsen diffusion has been related to electrode pore size for a ZrO_2 fuel cell [4]. The effects of diffusion and electrode porosity have been considered for protonic and oxygen-ion conducting solid electrolytes [5]. Gas kinetic theory has been applied to the analysis of a steam concentration cell that uses a high-temperature protonic solid electrolyte [6].

Discussions regarding fuel cells and related devices often assume or tacitly state that gas flow characteristics will have a negligible effect on electrical measurements. The purpose of this study has been to develop a set of parameters for assessing the effects of gas flow on fuel cell operation. For the case of static gas pressure, where no gas flow occurs, the system is described using kinetic theory and diffusion analyses. When flow occurs, parameters such as volume flow rates and Reynolds number characterize the dynamic gas.

2. Fuel cell principles

The voltage produced by a fuel cell, V_{cell}, is reduced from its open circuit or thermodynamic equilibrium value, V_e, by polarization mechanisms [7] according to the relation

$$V_{cell} = V_e - (V_{act} + IR + V_{conc}) \quad (1)$$

Here, V_{act} and V_{conc} represent activation and concentration polarization effects each occurring at the anode and cathode, while the term IR is the ohmic loss due to the electrolyte.

Rate-limiting processes of the ZrO_2 fuel cell have been discussed [8–10]. Although different electrode morphologies and experimental techniques made comparisons difficult, it was evident that both activation and concentration polarization mechanisms occurred.

Of interest in the present study is the concentration polarization term, which is given by

$$V_{conc} = \frac{R_g T}{n_e F} \ln\left(\frac{J_L}{J_L - J}\right) \quad (2)$$

3. Static gas

When there is no flow of gas the properties of the system can be described in terms of kinetic theory and diffusion [11].

3.1. *Kinetic theory*

The number of molecules striking a unit area of surface perpendicular to the incident direction per unit time is given by

$$z = \frac{n\bar{v}}{4} \quad (3)$$

where $\bar{v}$ is the average molecular velocity assuming a Maxwell–Boltzmann distribution. Equation 3 has been used [6] to infer that the species ionized at the anode of a steam concentration cell is water molecules rather than hydrogen molecules.

The mean free path between collision of like molecules, $\lambda_{1,1}$, and the diameter of rigid, elastic spherical molecules, δ, are related by the equation

$$\lambda_{1,1} = [(2)^{1/2}\pi n\delta^2]^{-1} \quad (4)$$

When the distribution of velocities and mean free paths are considered, the molecular diameter can be found from the gas viscosity, η, according to the relation

$$\eta = \frac{0.499m\bar{v}}{(2)^{1/2}\pi\delta^2} \quad (5)$$

The diameters of the molecules H_2, O_2 and N_2 are 2.68×10^{-8}, 3.65×10^{-8} and 3.78×10^{-8} cm, respectively.

For a mixture of two gases, the mean free path of one species between collisions with a second species is given by

$$\lambda_{1,2}^{-1} = \pi n_2 \delta_{1,2}^2 \left(1 + \frac{M_1}{M_2}\right)^{1/2} \quad (6)$$

and

$$\lambda_{2,1}^{-1} = \pi n_1 \delta_{1,2}^2 \left(1 + \frac{M_2}{M_1}\right)^{1/2} \quad (7)$$

where

$$n_i = \frac{P_i}{kT}; \quad i = 1, 2 \quad (8)$$

The mean free path for one species when colliding with either molecules of that species or with molecules of a second species is thus

$$\lambda_1^{-1} = 2^{1/2}\pi n_1 \delta_1^2 + \pi n_2 \delta_{1,2}^2 \left(1 + \frac{M_1}{M_2}\right)^{1/2} \quad (9)$$

and

$$\lambda_2^{-1} = 2^{1/2}\pi n_2 \delta_2^2 + \pi n_1 \delta_{1,2}^2 \left(1 + \frac{M_2}{M_1}\right)^{1/2} \quad (10)$$

where

$$\delta_{1,2} = \frac{\delta_1 + \delta_2}{2} \quad (11)$$

3.2. *Diffusion*

A concentration gradient, dN_v/dx, results in a molar flux, J_m, according to Fick's first law of diffusion

$$J_m = D\frac{dN_v}{dx} \quad (12)$$

The coefficient for the self-diffusion of like molecules has been shown [11] to be of the form

$$D_{1,1} = \frac{\bar{v}\lambda_{1,1}}{3} \quad (13)$$

For the interdiffusion of two gas species, the coefficient is

$$D_{1,2} = \frac{(\bar{v}_1^2 + \bar{v}_2^2)^{1/2}}{3\pi n\delta_{1,2}^2} \quad (14)$$

where

$$n = n_1 + n_2$$

If the mean free path between collisions is larger than the pore radius, r, of a porous material then Knudsen diffusion results, in which the diffusion coefficient is given by

$$D_k = \tfrac{2}{3}\bar{v}r, \quad r < \lambda \quad (15)$$

Table 1 shows order-of-magnitude electrode pore sizes for a number of electrochemical systems. Although the morphology of these structures has not been precisely or completely determined it can be seen that the range of pore or grain size (10^{-6} to 10^{-4} cm) is approximately that of the gas mean free path (10^{-5} to 10^{-4} cm). These gas parameters are given in Table 2.

The mean free paths, $\lambda_{1,1}$, for the anode and cathode reactant gases, hydrogen and oxygen respectively, were evaluated at 300° C and 0.1 atm according to Equation 7. When the reactant gases were mixed with a nitrogen carrier gas at each electrode, the mean free path for hydrogen and oxygen molecules when colliding with nitrogen molecules was determined from Equation 9; the partial pressures of the reactant and carrier gases were taken to be 0.1 and 0.9 atm, respectively. The mean free path of the reactant species when colliding with that species or with the carrier species was calculated from Equation 12, also at partial pressures of 0.1 and 0.9 atm.

Table 1. Electrode structures of electrochemical devices

Electrode morphology		*Application*	*Reference*
Structure	*Size (cm)*		
Pore	10^{-6}	Pt electrodes for ZrO_2 fuel cell	[4]
Pore	10^{-6} to 10^{-5}	Ni–Pr oxide electrodes for ZrO_2 fuel cell	[10]
Grain	2×10^{-5} to 10^{-4}	Pt electrodes for ZrO_2 fuel cell	[12]
Grain	2×10^{-4}	Pt electrodes for ZrO_2 fuel cell	[13]
Grain	10^{-5} to 10^{-4}	Pt electrodes for ZrO_2 fuel cell	[14]
Channel	10^{-4}	Ag electrode for ZrO_2/O_2 sensor	[15]
Pore	10^{-5}	Carbon electrodes for Li/SOCl battery	[16]

4. Dynamic gas

When a gas flows through a system the flow properties are determined by the flow regimen and geometry. The system considered here consists of a gas flowing through a cylindrical tube and incident upon a porous electrode as shown schematically in Fig. 1.

4.1. *Gas flow*

The Reynolds number is given by

$$Re = \frac{\varrho v d}{\eta} \tag{16}$$

The linear velocity is also the volume flow rate per unit of cross-sectional area, or

$$v = \frac{f}{A} \tag{17}$$

Thus, for a circular area of $A = \pi d^2/4$, the Reynolds number and flow rate are related as

$$Re = \frac{4\varrho f}{\pi d \eta} \tag{18}$$

The number of molecules incident on unit area perpendicular to the flow direction per unit time is given by

$$z' = \eta v \tag{19}$$

Therefore, from Equations 3, 17 and 19, the impingement ratio of incident molecules due to gas flow to those molecules resulting from average thermal velocity is

$$\frac{z'}{z} = \frac{4f}{A\bar{v}} \tag{20}$$

Values of z'/z and Re are shown in Table 3 for the anode and cathode gases flowing through a cylindrical tube of cross-sectional area of 1 cm^2. The first column gives the volume flow control rate, f', as measured by a mass flow controller under the standard conditions of 0° C and 1 atm in units of standard $cm^3 min^{-1}$. The second column shows the volume flow rate, f, at 300° C and 1 atm in $cm^3 s^{-1}$. It can be seen from Table 3 that the number of molecules incident at the electrode surface due to gas flow velocity is negligible with respect to those incident as a result of thermal motion until the flow becomes turbulent.

Table 2. Mean free paths of reactant gases

Anode – hydrogen reactant gas	*Cathode – oxygen reactant gas*
$\lambda_{1,1} = 2.54 \times 10^{-4}$	$\lambda_{1,1} = 1.32 \times 10^{-4}$
$\lambda_{1,2} = 2.56 \times 10^{-5}$	$\lambda_{1,2} = 1.36 \times 10^{-5}$
$\lambda_1 = 2.32 \times 10^{-5}$	$\lambda_1 = 1.23 \times 10^{-5}$

5. Electrochemical processes

The conversion of a gas to electrical current involves four fundamental processes: (i) the flow of gas to the electrode; (ii) the diffusion of gas through the electrode to the electrochemical reaction site; (iii) catalytic reactions, which may include surface diffusion; and (iv) ionic conduction through the electrolyte. In the first step, the current can be related [17] to the gas-volume flow rate by utilizing the ideal gas law, the definition of the volume flow rate, $f = v/t$, and

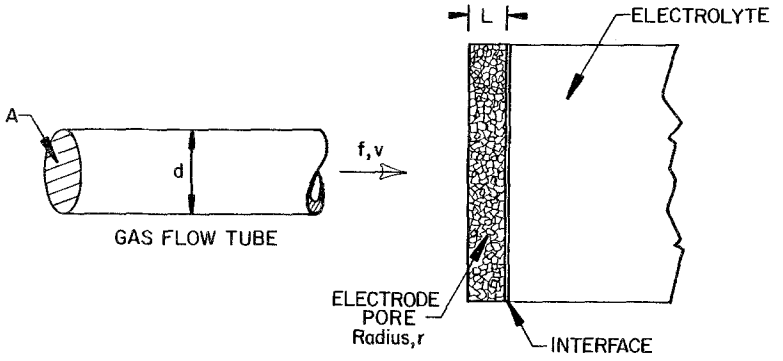

Fig. 1. Schematic diagram of gas flow to electrode.

Faraday's law

$$Q = \int_0^t I dt = nNF \tag{21}$$

From these relations it follows that

$$f = \frac{R_g T}{P_i} \frac{I}{nF} \tag{22}$$

The limiting electrical current density for gas diffusion is given by

$$J_L = n_e F J_m \tag{23}$$

where the molar flux now contains a term for the electrode porosity, p, and tortuosity, τ

$$J_m = \frac{D}{R_g T} \frac{dP_i}{dx} \frac{p}{\tau} \tag{24}$$

At the anode, the reaction is of the type

$$H_2 \longrightarrow 2H^+ + 2e \tag{25}$$

so that $n = 2$; and at the cathode, the reaction is

$$O_2 + 4e \longrightarrow 2O^{2-} \tag{26}$$

where $n = 4$. The diffusion coefficient, D is determined by the particular process and involves mechanisms such as self-diffusion, interdiffusion of a reactant gas in an inert carrier gas, or Knudsen flow. The pressure differential, dP, is the difference between the ambient pressure at the outer surface of the electrode and the pressure at the electrochemical reaction site, which is assumed to be located near the interface between the electrode and the electrolyte.

Table 4 gives the diffusion coefficients and limiting current densities for the major processes occurring at the anode and cathode. The diffusion coefficients are found from Equations 13, 14 and 15. In each case, the partial pressures of the reactant and carrier gases are taken to be 0.1 and 0.9 atm, respectively; the temperature is 300° C.

Table 3. Gas flow parameters

Flow rates		*Anode gas, hydrogen*			*Cathode gas, oxygen*		
f′ *at 0° C, 1 atm (standard* $cm^3 min^{-1}$)	f *at 300° C, 1 atm* ($cm^3 s^{-1}$)	z′/z	Re	*Flow type*	z′/z	Re	*Flow type*
0.286	10^{-2}	1.63×10^{-7}	3.77×10^{-3}	Laminar	6.50×10^{-7}	2.78×10^{-2}	Laminar
2.86	10^{-1}	1.63×10^{-6}	3.77×10^{-2}		6.50×10^{-6}	2.78×10^{-1}	
28.6	1	1.63×10^{-5}	3.77×10^{-1}		6.50×10^{-5}	2.78	
286	10	1.63×10^{-4}	3.77		6.50×10^{-4}	27.8	
2.86×10^3	10^2	1.63×10^{-3}	37.7		6.50×10^{-3}	278	
2.86×10^4	10^3	1.63×10^{-2}	377		6.50×10^{-2}	2.78×10^3	Turbulent
2.86×10^5	10^4	1.63×10^{-1}	3.77×10^3	Turbulent	6.50×10^{-1}	2.78×10^4	
2.86×10^6	10^5	1.63	3.77×10^4		6.50	2.78×10^5	

Table 4. Diffusion coefficients and limiting current densities of reactant gases

Anode, Hydrogen reactant gas, 300° C		*Cathode, Oxygen reactant gas, 300° C*	
Diffusion coefficient ($cm^2 s^{-1}$)	*Limiting current density* ($A\,cm^{-2}$)	*Diffusion coefficient* ($cm^2 s^{-1}$)	*Limiting current density* ($A\,cm^{-2}$)
$D_{1,1} = 2.00$	$J_{1,1} = 82.0$	$D_{1,1} = 0.271$	$J_{1,1} = 22.2$
$D_{1,2} = 2.02$	$J_{1,2} = 82.9$	$D_{1,2} = 0.540$	$J_{1,2} = 44.3$
$r = 10^{-5}$ cm; $D_k = 1.64$	$r = 10^{-6}$ cm; $J_k = 6.71$	$r = 10^{-6}$ cm; $D_k = 0.0411$	$r = 10^{-6}$ cm; $J_k = 3.37$
$r = 10^{-5}$ cm; $D_k = 1.64$	$r = 10^{-5}$ cm; $J_k = 67.1$	$r = 10^{-5}$ cm; $D_k = 0.411$	$r = 10^{-5}$ cm; $J_k = 33.7$
$D_b \simeq 10^{-5}$	$J_b \simeq 10^{-2}$	$D_b \simeq 10^{-9}$	$J_b \simeq 10^{-5}$

For each diffusion mechanism the limiting current density is determined according to Equations 23 and 24. The partial pressure gradient is assumed to be 0.1 atm across an electrode of thickness $L = 10^{-3}$ cm (10 μm). The ratio p/τ [4] is given a value of 0.1.

The values of diffusion coefficient and limiting current density may be compared with those resulting from the bulk diffusion of gas through a non-porous metal layer. The diffusion coefficient [18] of hydrogen in palladium, iron and nickel at 300° C ranges between 10^{-6} and $10^{-4}\,cm^2\,s^{-1}$ so that a representative value of 10^{-5} can be assumed. The diffusion coefficient [19] of oxygen in platinum is $\simeq 10^{-9}\,cm^2\,s^{-1}$ at 1400° C. These coefficients together with reactant gas partial pressures of 1 atm and a non-porous electrode thickness of 10^{-3} cm result in limiting current densities of $\simeq 10^{-2}$ and $10^{-5}\,A\,cm^{-2}$ for hydrogen and oxygen, as shown in Table 4.

From Equations 22–24, the ratio of impingement rates and Reynolds number can be evaluated for the reactant gases flowing through a cylindrical tube of cross-section 1 cm^2. With the largest values of limiting current densities shown in Table 4, i.e. 82.9 and 44.3 $A\,cm^{-2}$ for hydrogen and oxygen, z'/z and Re are found to be 3.29×10^{-3} and 76 for hydrogen; the corresponding quantities for oxygen are 3.51×10^{-3} and 150. Thus, even at these extreme current densities, the gas flow effects are minimal.

The limiting current densities shown for gas diffusion processes in Table 4 may be compared with those resulting from activation polarization of the electrode–electrolyte interface region and from ohmic polarization of the electrolyte. The exchange current density, which occurs at zero bias has been estimated [20] to be of the order of $10^{-3}\,A\,cm^{-2}$ for protonic systems. For an electrolyte with an ionic conductivity of 10^{-2} $(\Omega\,cm)^{-1}$ and a cell voltage of 1 V across a sample 0.1 cm thick, the resulting current density is $10^{-1}\,A\,cm^2$.

6. Conclusions

The properties of a static gas and a dynamic gas have been evaluated and related in terms of fuel cell applications. The impingement ratio, z'/z, becomes important only as the flow becomes turbulent. Turbulent flow is not necessary because flow rates greatly in excess of the electrochemical conversion rate can be maintained with laminar flow.

The ratio, z'/z, also indicates that the impingement direction of the incident gas molecules relative to the electrode surface is not important at low or moderate flow rates. From this observation it can be inferred that disc or tubular fuel cell geometry will not be significantly affected by gas flow considerations.

The electrode pore size range for a protonic electrolyte fuel cell is likely to be 10^{-6} to 10^{-4} cm (0.01 to 1 μm). With this morphology, self-diffusion of a single gas species or interdiffusion of a mixed gas species can be expected for $r > \lambda$. Knudsen diffusion will occur when $r < \lambda$.

Concentration polarization will not be the rate-limiting step of the fuel cell if the electrodes are moderately porous, i.e. $p \simeq 10\%$. This limitation will occur as a result of activation polarization at the electrode–electrolyte interface or by ohmic polarization of the electrolyte.

Acknowledgement

References

[1] A. K. Kuriakose, T. A. Wheat, A. Ahmad and J. Dirocco, *J. Amer. Ceramic Soc.* **67** (1983) 179.

[2] A. Ahmad, T. A. Wheat, A. K. Kuriakose and B. Kindl, *J. Can. Ceramic Soc.* **52** (1983) 1.

[3] A. K. Kuriakose, T. A. Wheat and A. Ahmad, in 'Progress in Solid Electrolytes' (edited by T. A. Wheat, A. Ahmad and A. K. Kuriakose), Energy, Mines and Resources, Canada (1983).

[4] S. Pizzini, M. Bianchi, P. Colombo and S. Torchio, *J. Appl. Electrochem.* **3** (1973) 153.

[5] E. J. L. Schouler, M. L. S. Birchall and J. S. Lundsgaard, in 'Solid State Protonic Conductors I' (edited by J. Jensen and M. Kleitz), Odense University Press, Odense, Denmark (1982).

[6] H. Uchida, N. Maeda and H. Iwahara, *J. Appl. Electrochem.* **12** (1982) 645.

[7] A. McDougall, 'Fuel Cells', John Wiley and Sons, New York (1976).

[8] B. C. H. Steele, in 'Electrode Processes in Solid State Ionics' (edited by M. Kleitz and J. Dupuy), D. Reidel Publ. Co., Dordrecht, Holland (1976).

[9] T. M. Gur, I. D. Raistrick and R. A. Huggins, *J. Electrochem. Soc.* **127** (1980) 2620.

[10] C. Mari, V. Scolari, G. Fiori and S. Pizzini, *J. Appl. Electrochem.* **1** (1977) 95.

[11] A. Roth, 'Vacuum Technology', North-Holland Publishing Co., Amsterdam (1976).

[12] Da Yu Wang and A. S. Nowick, *J. Electrochem. Soc.* **128** (1981) 55.

[13] D. Braunshtein, D. S. Tannhauser and I. Ries, *ibid.* **128** (1981) 82.

[14] M. J. Verkerk, M. W. J. Hammink and A. J. Burggraaf, *ibid.* **130** (1983) 70.

[15] T. Arakawa, A. Saito and J. Shiokawa, *Appl. Surface Sci.* **16** (1983) 365.

[16] S. Szpak and J. R. Driscoll, *J. Power Sources* **10** (1983) 343.

[17] D. Pletcher, 'Industrial Electrochemistry', Chapman and Hall, London (1982).

[18] N. A. Galaktionowa, 'Hydrogen–Metal Systems Databook', Ordentlich Publishers, Holon, Israel (1980).

[19] L. R. Velho and R. W. Bartlett, *Metall. Trans.* **3** (1972) 65.

[20] M. F. Bell, M. Sayer, P. S. Nicholson and K. Yamashita, Presented at the Hydrogen Energy Conference, Toronto (1984).